Terlau, Marina ; von Freyberg, Axel ; Stöbener, Dirk ; Fischer, Andreas

In-Process Tool Deflection Measurement in Incremental Sheet Metal Forming

Conference paper as: peer-reviewed accepted version (Postprint)

DOI of this document*(secondary publication): https://doi.org/10.26092/elib/3649

Publication date of this document: 07/02/2025

* for better findability or for reliable citation

Recommended Citation (primary publication/Version of Record) incl. DOI:

M. Terlau, A. von Freyberg, D. Stöbener and A. Fischer, "In-Process Tool Deflection Measurement in Incremental Sheet Metal Forming," 2022 IEEE Sensors Applications Symposium (SAS), Sundsvall, Sweden, 2022, pp. 1-6, doi: 10.1109/SAS54819.2022.9881345.

In-Process Tool Deflection Measurement in Incremental Sheet Metal Forming

1st Marina Terlau
University of Bremen
Bremen Institute for Metrology, Automation and Quality Science (BIMAQ)
Bremen, Germany
m.terlau@bimaq.de, 0000-0002-5698-7049

2nd Axel von Freyberg
University of Bremen
Bremen Institute for Metrology, Automation and Quality Science (BIMAQ)
Bremen, Germany
a.freyberg@bimaq.de, 0000-0002-0936-3655

3rd Dirk Stöbener
University of Bremen
Bremen Institute for Metrology, Automation and Quality Science (BIMAQ)
Bremen, Germany
d.stoebener@bimaq.de, 0000-0002-1624-2106

4th Andreas Fischer
University of Bremen
Bremen Institute for Metrology, Automation and Quality Science (BIMAQ)
Bremen, Germany
andreas.fischer@bimaq.de, 0000-0001-7349-7722

***Abstract*—Incremental sheet forming is an economical alternative to deep drawing for forming large sheets in small quantities. However, the shape deviations resulting from a process-force-caused tool deflection limits the measuring accuracy. Therefore, an optical multi-sensor system is proposed to enable the contactless in-process measurement of the tool deflection independent of the machine kinematics for the first time. The presented design study of the sensor system aims to meet the requirement of a maximal measurement uncertainty of 15 µm at a measuring distance of up to 2 m. The multi-sensor system consists of a large number of inexpensive angulation sensors, each of which measures an angle to a light source on the tool. Based on the measured angles of all sensors calibrated to each other, the position of the tool in the three-dimensional manufacturing volume can be calculated by multi-angulation. Via experimental characterization of a realized angulation sensor as well as an uncertainty propagation, the measurement uncertainty achievable with the overall system is estimated. As a result, the multi-sensor concept fulfills all requirements for the measurement of the tool deflection in incremental sheet metal forming.**

***Index Terms*—incremental sheet forming, shadow imaging, multi-angulation**

I. Introduction

For the production of large sheet metal parts in small batches, incremental sheet metal forming is an economical alternative to conventional forming processes due to the inexpensive and flexible tools [1]. The disadvantages of incremental sheet metal forming are geometry deviations due to springback of the sheet [2] and deflections of the forming tool [3]. In order to compensate for tool deflection, the deflection must be determined. However, a prediction of the tool deflection based on mechanical calculations [4] is based on model assumptions and takes neither machine tool errors nor the deformations of the machine into account. Therefore, a measurement of the tool deflection is required that is independent of these limitations and thus allows for lower uncertainty.

The IGF project No. 290 EBG has been funded via the AiF within the transnational CORNET program by the Federal Ministry of Economics and Climate Protection based on an enactment of the German Parliament.

It also should be able to measure in-process and close to the tool contact point as well as contactless and independent of the machine tool kinematics. Therefore, the possible approaches are narrowed down to optical systems. With respect to the specific application, the measurement of tool deflection in an incremental sheet forming machine, a measuring volume of 2.0 x 1.0 x 0.2 m³ has to be covered. Assuming a usual tool deflection of 150 µm to 450 µm [4], a position measurement uncertainty of 15 µm is required according to the golden rule of metrology. This means a dynamic measuring range $> 10^5$, which results from the quotient of measuring range and the required uncertainty.

A. State of the art

While the required dynamic measuring range cannot be achieved with full-field photogrammetry [5], multisensor measuring systems offer the possibility of detecting the tool position in the measuring volume by means of multi-angulation or multilateration, depending on the measuring principle of the sensors used.

Optical distance sensors suitable for multilateration usually have a lateral measuring range that is too small for the planned application. Tracking systems based on interferometric sensors, e. g. Lasertracker [6], contain a control system to enable an active movement for tracking the target point. However, if the line of sight is interrupted during the machine movement, the measurement fails. Current scanning systems cannot achieve a scan time per measurement point of less than 300 µs, which is required to avoid motion blur at a common

feed rate of 50 mm/s [7]. Multilateration measuring systems are therefore unsuitable for the planned application.

By means of multi-angulation of a light source, the required axial and lateral measuring range can be realized in principle. The light source, which can be attached to the tool tip, casts a shadow through a coded mask onto a camera, which is why the principle is also called shadow imaging [8]. From the position of the shadow image, the observation angle to the light source can finally be inferred. Additionally, shadow imaging sensors enable an estimation of the distance to the light source based on an evaluation of the image magnification [9]. In contrast to conventional imaging, the information is distributed over the whole image and not concentrated on a few pixels, which allows averaging and thus a reduction of the measurement uncertainty.

Various image evaluation algorithms have been established for calculating the position or displacement of the shadow image. If the pattern contains periodic elements, the phase shift can be used to determine the image shift [10], [11]. Furthermore, a correlation algorithm is applicable for computing the image shift [12], and Yu et al. [13] have implemented a quadratic approximation for locating the stripes. Previous studies demonstrate an achievable image shift standard uncertainty of $\frac{1.5}{1000}$ px [12] and $\frac{4.9}{1000}$ px [11], respectively. The subpixel resolution demonstrated here, underlines the high potential regarding the angular resolution of the shadow image principle.

In summary, a multi-angulation measurement system (MAM) based on shadow imaging is a promising approach to measure tool deflection. However, it remains to be clarified whether or in which measurement volume the required measurement uncertainty of the tool deflection can be achieved. Furthermore, it has to be investigated whether a single sensor is capable of an axial position measurement with a sufficient uncertainty or whether a second sensor is required to determine the distance by triangulation.

B. Objective and outline

The aim of this work is to estimate the position measurement uncertainty achievable with a single shadow imaging sensor with respect to its application in an MAM for the measurement of tool deflection in incremental sheet metal forming. For this purpose, the measurement uncertainty of one sensor is examined in angular and axial direction.

Section II introduces the principle of measurement. Section III describes the experimental setup and the applied image processing. The achievable measurement errors considering the determination of the image position, the distance measurement and the calculation of the tool position are presented and discussed in Section IV. Finally, Section V contains a conclusion (also regarding the overall multi-sensor system) and an outlook.

II. Measuring principle

A single sensor used in an MAM to measure tool deflection during incremental sheet metal forming is composed of a camera chip and a shadow mask, i. e. a planar structure containing translucent and opaque portions. In addition, a light source is attached to the tool tip to be detected.

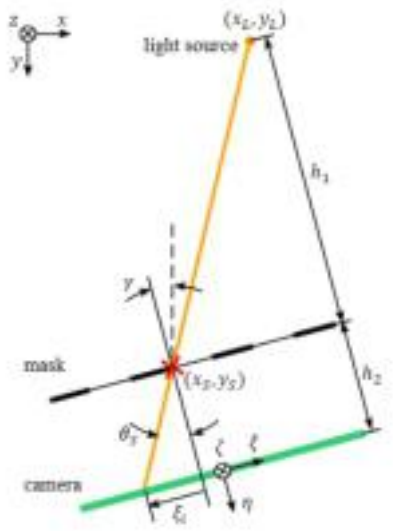

Fig. 1. Measuring principle of the shadow-based angulation sensor. The position of a light source (x_L, y_L) in the machine coordinate system (x, y, z) at distance h_1 from the shadow mask leads to a position of the shadow image ξ_i in the sensor coordinate system (ξ, η, ζ) on the sensor at distance h_2 from the shadow mask.

Since the deflection of the forming stylus mainly occurs in the horizontal plane [4], this paper focuses on the measurement of the position components in the horizontal (x, y) plane in the machine coordinate system (MCS). The shadow imaging sensor measures an angle to the light source so that the position of the sensor (x_S, y_S) and the measured angle Θ_M in the MCS span the straight line on which the light source is located. Either the measured distance or the angle measurement of another sensor provides the parameter s_L and thus defines the position of the light source, which can be written in the following form:

$$\begin{bmatrix} x_L \\ y_L \end{bmatrix} = \begin{bmatrix} x_S \\ y_S \end{bmatrix} + s_L \cdot \begin{bmatrix} \sin(\Theta_M) \\ \cos(\Theta_M) \end{bmatrix}. \tag{1}$$

The straight line orientation in the MCS

$$\Theta_M = \Theta_S - \gamma \tag{2}$$

is composed of the angle Θ_S measured by the sensor and the angle γ by which the (ξ, η, ζ)-sensor coordinate system (SCS) is rotated around the ζ-axis with respect to the MCS. Rotation about the ξ-axis does not affect the straight line orientation in the MCS. A rotation around the η-axis is to be avoided as far as possible when aligning the sensor and enters the coordinate transformation with the cosine of the angle, so that this angle can be neglected.

The angle Θ_S is the intermediate quantity that the individual sensor delivers for the angular direction. The underlying principle is visualized in Fig. 1. A light source casts a shadow through the shadow mask onto the image sensor in the (ξ, ζ)-image plane of the SCS, so that the shadow image of any point

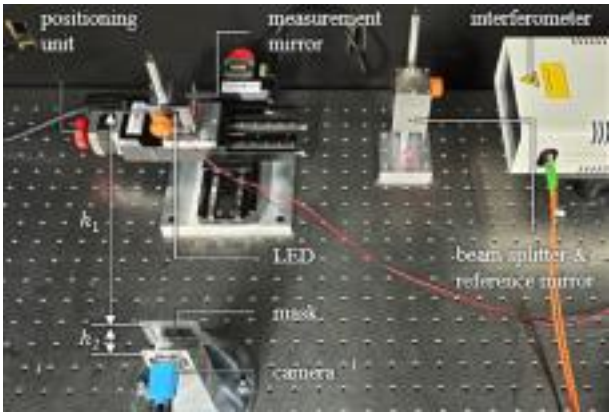

Fig. 2. Experimental setup for the experimental investigation of the uncertainty of the image displacement measurement.

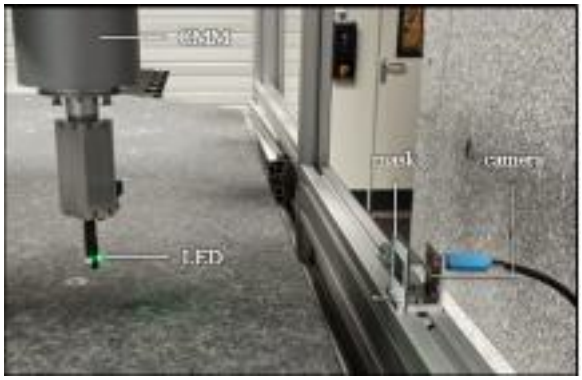

Fig. 3. Experimental setup for experimental validation of the measurement system.

on the shadow mask appears at the image position ξ. Provided that $\xi = 0$ is defined where the light source is exactly centered in front of the sensor, the angle measured by the sensor

$$\Theta_S = \arctan\left(\frac{\xi_i}{h_2}\right) \tag{3}$$

is calculated from the image position ξ_i and the distance h_2 between mask and sensor. The image position is determined by processing the images captured with the camera chip.

The axial position component is determined by evaluating the magnification of the mask. The distance from the shadow mask to the light source

$$h_1 = \frac{l_M \cdot h_2}{l_S - l_M} \tag{4}$$

is calculated from the length of a feature in the mask l_M, its length projected to the sensor l_S and the distance between sensor and mask h_2. The feature length on the sensor is extracted from the captured images.

III. Experimental setup

A. Setup of the measuring system

For experimental validation of the angular measurement with a shadow imaging sensor, the experimental setup shown in Fig. 2 is used. A positioning unit is used to move a surface mounted device - light emitting diode (SMD-LED) with a peak wavelength of 518 nm laterally to the sensor's viewing direction, which corresponds to the movement and deflection of the forming tool during incremental sheet metal forming, to which an LED is attached near the tool tip. A laser interferometer is used for reference measurement of the displacement of the LED, which is mounted on the measuring mirror.

To ensure the most ideal conditions possible, a darkening setup prevents interference from ambient light. The angulation sensor is positioned so that the distance between the mask and the LED is $h_1 = 227$ mm. The mask used for the angulation sensor contains transparent and non-transparent, vertically oriented strips. The width of the transparent strips is 80 µm. Among the intransparent stripes, every fifth stripe with 181 µm has a larger width than the others, which are 170 µm wide. The DMM 37UX273-ML monochrome board camera from the company The Imaging Source, located about 20 mm (distance h_2) behind the mask, contains a CMOS sensor with 1440 × 1080 quadratic pixels, each 3.45 µm in size.

In order to determine the uncertainty of the image shift with this setup, the LED is moved stepwise by 200 µm over a total distance of 60 mm by the positioning unit. During this process, the camera takes an image after each step, so that there is one image for each of all 300 positions.

To experimentally validate the distance measurement with the shadow imaging sensor, the setup presented in Fig. 3 is used. The SMD-LED is attached to a coordinate measuring machine (CMM). The CMM moves the LED in axial direction to the sensor and serves as a reference measuring system to determine the LED position.

The experiment is conducted in a dark laboratory to avoid influences due to environmental illumination. The same mask and camera as in the previously described setup are used.

For investigating the sensor's axial measurement capabilities, the CMM moves the LED to positions in distances to the sensor between 100 mm and 600 mm. LED positions are arranged axially in front of the sensor and each 500 µm apart. At each LED position, the sensor records ten images to demonstrate the sensor's principle behavior and to evaluate the uncertainty for distance measurement.

B. Image processing

By means of image processing, the image position and the stripe spacing used for distance calculation is evaluated. The image position results from a continuous cumulation of image displacements, that can be determined by comparing two sequential images. To determine the image displacement and the stripe spacing, the stripes are approximated with a model function, which is a limited Gaussian function that corresponds to the intensity distribution of a stripe. The first step in the implementation of the approximation is a preprocessing of the data, where a low-pass filter is used to smooth the column-averaged intensity distribution. Then, the

limited Gaussian function is fitted to the intensity distribution of each white stripe. In the used model function

$$I_M(\xi) = \begin{cases} I_0 + A \cdot e^{-\left(\frac{|\xi-\mu|}{w}\right)^2} & \text{for } I(\xi) < I_{max} \\ I_{max} & \text{for } I(\xi) \geq I_{max} \end{cases}, \quad (5)$$

I_0 describes the intensity minimum, A the amplitude of the function, i. e. the difference between maximum and minimum, μ the position of the maximum within the intensity cutout and w the width of the Gaussian curve. The limitation value I_{max} limits the height of the Gaussian function so that the peak is flattened. The approximation of the model function to the intensity slope provides the parameters of the model function and thus the position of the maximum μ. By that, a position can be defined for each white stripe in the image. The displacement of the white stripes can be determined in two sequential images, and then, the image displacement follows from the averaging of the stripe displacements. From the determined stripe positions in one image, the stripe spacing for the distance evaluation is derived. The stripe spacing is averaged for all short spacings corresponding to the smaller intransparent stripes.

IV. Results and discussion

A. Measuring the image displacement

Based on the experimentally recorded images, the image shift between successive images can be determined using the presented evaluation algorithms. If the light source moves parallel to the sensor, the image shift is

$$\Delta\xi = -\frac{h_2}{h_1} \cdot \Delta L \quad (6)$$

proportional to the displacement ΔL of the light source, where h_2 is the distance between sensor and mask and h_1 is the constant axial distance between mask and light source (cf. Fig. 1). Via the proportional relationship, the interferometrically measured LED shift can be used as a reference measurement to determine the uncertainty of the image shift, although the determination of the image shift is done in the image plane while the interferometer measures the real LED shift. Since the distances are not ideally known, the determination of the constant scaling factor

$$p = -\frac{h_2}{h_1} = \frac{\overline{\Delta\xi}}{\overline{\Delta L}} \quad (7)$$

is based on the mean values of the LED displacement $\overline{\Delta L}$ and the image displacement $\overline{\Delta\xi}$. In reality, however, the LED does not move ideally parallel to the sensor plane, which causes the image offsets to be larger on one side of the 60 mm total travel distance than on the other. The slope in the image displacement values is determined by linear regression, and then, the image displacements are corrected so that the slope is zero. During correction, the mean value of the image displacement is maintained. The transformations allow a comparison between the image displacement measured by the angulation sensor and the LED displacement measured by the interferometer. Thus, the mean squared deviation of the image shift

$$u^2(\Delta\xi) = \frac{1}{n-1}\sum_{i=1}^{n}(\Delta\xi_c - \Delta L_s)^2 \quad (8)$$

is calculated from all n measured values of the corrected image shift $\Delta\xi_c$ and the scaled LED shift $\Delta L_s = p{\cdot}\Delta L$, which serves as reference value. The root of the mean squared deviation is used as a measure of the standard uncertainty of the image displacement, which amounts to 23 nm or accordingly $\frac{6.7}{1000}$ px in the presented experiment. Thus, the image displacement uncertainty is in the same order of magnitude as in the state of the art.

B. Distance measurement

In order to determine the distance of the LED to the sensor, the mean stripe spacing is evaluated from the captured images. The calculation of distance h_1 can be conducted based on (4). However, the stripe spacing is not ideally known and not identical for all periods due to manufacturing deviations. Consequently, the uncertainty of the stripe spacing in the mask l_M propagates to a distance uncertainty

$$u^2_{l_M}(h_1) = \left(\frac{\partial h_1}{\partial l_M}\right)^2 \cdot u^2(l_M) \quad (9)$$

by multiplication with the sensitivity of the LED distance to the stripe spacing based on (4). The analytically determined sensitivity combined with an uncertainty of stripe spacing in the mask of $u(l_M) = 0.5$ µm leads to a distance uncertainty of $u_{l_M}(h_1 = 200\ mm) = 4$ mm. The calculated distance uncertainty shows that the distance measurement based on the model equation is unsuitable for tool deflection measurement.

For practical application of the shadow imaging sensor for distance measurement, a calibration curve can be used to circumvent the influence of slightly varying stripe width on the distance measurement. To capture the calibration curve, first, the mean stripe spacing l_S is evaluated for each image. Second, the mean stripe spacing is averaged for all ten images per LED position. The averaged stripe spacing is then assigned to the LED distances h_1 measured by the CMM, which is shown in Fig. 4. The resulting assignment provides the calibration curve by interpolation. The stripe spacing decreases as the distance increases, i. e. it is more sensitive to distance variations for smaller distances. This is in accordance to the theoretical model (4), which is fitted to the data and included in Fig. 4.

To estimate the best achievable uncertainty for the distance measurement based on the captured calibration curve, the calibration curve is applied to determine the distances of the LED for each recorded image. This means, for the evaluated stripe spacing of an image, the distance of the LED to the sensor is interpolated from the calibration data. The difference between the interpolated distance and the given distance by the CMM provides the error of the distance measurement for each image. So, for each distance, the root of the mean squared error of the ten samples is used as the distance depending uncertainty of the distance measurement.

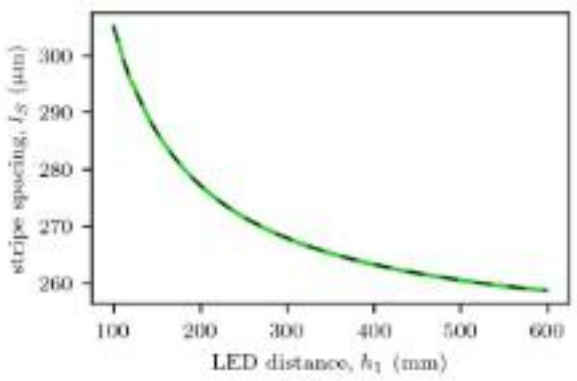

Fig. 4. Calibration curve showing the relation between the evaluated stripe spacing l_S and the LED distance from the sensor h_1. The measured data (green markers) is compared with the fitted model (dashed line) from (4).

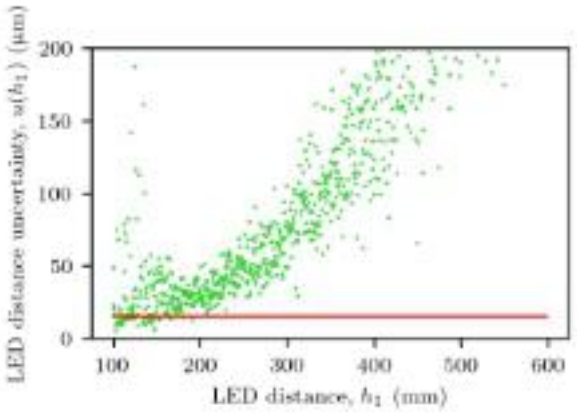

Fig. 5. Experimentally evaluated uncertainty of the measured distance between sensor and LED h_1. The red line marks the required position uncertainty limit of 15 µm

This uncertainty of the distance measurement is presented in Fig. 5. In the average, the uncertainty of the distance rises with an increasing distance. The distance depending uncertainty increase corresponds with the calibration curve, that shows that a low variation of the stripe spacing results in higher variations of the distance with increasing distance. Additionally, there are outliers at distances shorter than 140 mm which come along with scattering stripe spacings in the images at corresponding LED-positions. In total, less than 5 % of the sample LED positions provide a distance measurement uncertainty of less than the required position uncertainty of 15 µm. Therefore, the measurement uncertainty in axial direction is insufficient for tool deflection measurement in incremental sheet metal forming. Consequently, the shadow imaging sensor is only considered as an angular sensor and the distance is calculated by triangulation of at least two sensors.

C. Uncertainty of the LED position

For the measurement of tool deflection in incremental sheet metal forming, the uncertainty of the position measurement of the LED attached to the tool tip is of interest. The position uncertainty can be determined from the uncertainty propagation for the model equation (1). The uncertainty of the image displacement is equivalent to the uncertainty of the image position ($u(\xi) = u(\Delta\xi)$), since the absolute position is obtained by adding the evaluated displacements and the known reference position. To characterize a single sensor, s_L is assumed to be ideally known. Thus, the position of the LED

$$(x_L, y_L) = f(x_S, y_S, \gamma, h_2, \xi_i) \tag{10}$$

depends on the calibration variables sensor position (x_S, y_S), sensor orientation γ and distance h_2 between shadow mask and camera sensor as well as the image position ξ_i, according to (1) to (3).

According to the uncertainty propagation calculation, the uncertainties are assigned to the position components

$$\begin{aligned} u^2(x_L) = &\left(\frac{\partial x_L}{\partial x_S}\right)^2 \cdot u^2(x_S) + \left(\frac{\partial x_L}{\partial \gamma}\right)^2 \cdot u^2(\gamma) \\ &+ \left(\frac{\partial x_L}{\partial h_2}\right)^2 \cdot u^2(h_2) + \left(\frac{\partial x_L}{\partial \xi_B}\right)^2 \cdot u^2(\xi_i) \end{aligned} \tag{11}$$

and

$$\begin{aligned} u^2(y_L) = &\left(\frac{\partial y_L}{\partial y_S}\right)^2 \cdot u^2(y_S) + \left(\frac{\partial y_L}{\partial \gamma}\right)^2 \cdot u^2(\gamma) \\ &+ \left(\frac{\partial y_L}{\partial h_2}\right)^2 \cdot u^2(h_2) + \left(\frac{\partial y_L}{\partial \xi_B}\right)^2 \cdot u^2(\xi_i) \end{aligned} \tag{12}$$

is calculated from the sensitivities of the position components to the influence quantities and the uncertainties of the influence quantities. To calculate the position uncertainty, the sensitivity coefficients (the partial derivatives) are determined analytically from (1) to (3). The uncertainties of the calibration quantities are estimated and the results of the experimental investigation are used for the uncertainty of the image position. For the quantitative uncertainty determination, the uncertainty of the distance between the mask and the sensor is assumed to be $u(h_2) = 1$ µm, the uncertainty of the sensor orientation is assumed to be $u(\gamma) = 30$ µrad, and the uncertainties of the sensor position components are assumed to be $u(x_S) = u(y_S) = 3$ µm. The experimentally achieved standard uncertainty of the image displacement of $u(\xi_i) = 23$ nm is used as the image position uncertainty.

From the uncertainty propagation follows the standard uncertainty shown in Fig. 6 as a function of the position of the light source. The uncertainty increases with increasing axial and lateral distance from the sensor. Accordingly, the required position uncertainty can only be achieved up to a distance of about 480 mm. This means that in order to cover the entire working range of the machine tool with a sufficient position uncertainty, several sensors must be used, each measuring a part of the working range. In addition, triangulation with two sensors in the center of the machine tool is not sufficient, so that the data of several angulation sensors must be calculated in this area.

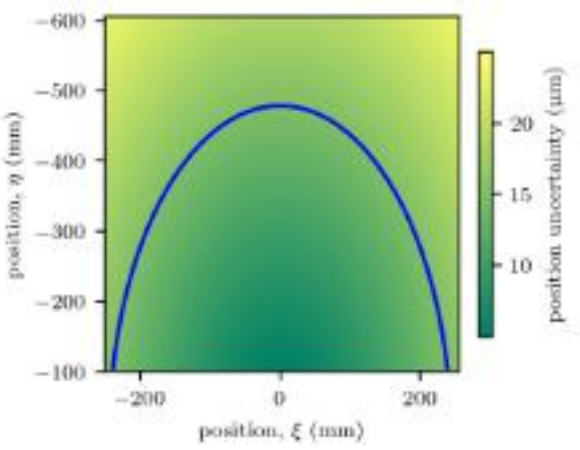

Fig. 6. Spatial distribution of the uncertainty of the light source position. The blue contour highlights the required limit of 15 µm.

V. Conclusion and Outlook

For in-process measurement of the deflection of the forming tool during incremental sheet metal forming, a position measurement uncertainty of 15 µm is required. This is to be realized with a multi-sensor system based on shadow-based angulation sensors. The contribution of a single sensor to the position measurement uncertainty was therefore investigated in the present article.

The experimental investigations prove that the shadow imaging sensor is suitable for the angular (i. e. the lateral) position measurement but its axial position measurement uncertainty is insufficient. Therefore, further sensors are needed for distance calculation via triangulation, which increases the effective aperture and thus reduces the uncertainty. Based on the experimental determination of the image position uncertainty and the estimation of further uncertainty contributions, it is finally shown that the required position measurement uncertainty is generally achievable with the proposed measuring principle.

In current and future work, the influence of ambient light as well as the uncertainty contributions of the calibration quantities and an optimal calibration strategy will be investigated. Further studies are planned to understand the achievable position uncertainty with an increasing number of sensors.

References

[1] A. Kumar and V. Gulati, "Experimental investigations and optimization of forming force in incremental sheet forming," *Sādhanā*, vol. 43, no. 10, p. 42, 2018.

[2] H. Ren, J. Xie, S. Liao, D. Leem, K. Ehmann, and J. Cao, "In-situ springback compensation in incremental sheet forming," *CIRP Annals*, vol. 68, no. 1, pp. 317–320, 2019.

[3] P. Konka, R. Lingam, U. A. Singh, C. Shivaprasad, and N. V. Reddy, "Enhancement of accuracy in double sided incremental forming by compensating tool path for machine tool errors," *The International Journal of Advanced Manufacturing Technology*, vol. 111, no. 3-4, pp. 1187–1199, 2020.

[4] P. Konka, R. Lingam, and N. V. Reddy, "Tool path design system to enhance accuracy during double sided incremental forming - an analytical model to predict compensations for small/large components," *Journal of Manufacturing Processes*, vol. 58, pp. 510–523, 2020.

[5] D. Sims-Waterhouse, M. Isa, S. Piano, and R. Leach, "Uncertainty model for a traceable stereo-photogrammetry system," *Precision Engineering*, vol. 63, pp. 1–9, 2020.

[6] U. Mutilba, J. A. Yagüe-Fabra, E. Gomez-Acedo, G. Kortaberria, and A. Olarra, "Integrated multilateration for machine tool automatic verification," *CIRP Annals*, vol. 67, no. 1, pp. 555–558, 2018.

[7] A. Kumar, V. Gulati, and P. Kumar, "Investigation of process variables on forming forces in incremental sheet forming," *International Journal of Engineering and Technology*, vol. 10, no. 3, pp. 680–684, 2018.

[8] P. Masa, E. Franzi, and C. Urban, "Nanometric resolution absolute position encoders," in *Proceedings of 13th European Space Mechanisms and Tribology Symposium*, ESA, Ed., 2009.

[9] E. Grenet, P. Masa, E. Franzi, and D. Hasler, "Measurement system of a light source in space," Patent EP2 593 755, 2015.

[10] A. N. Andre, P. Sandoz, B. Mauze, M. Jacquot, and G. J. Laurent, "Sensing one nanometer over ten centimeters: A microencoded target for visual in-plane position measurement," *IEEE/ASME Transactions on Mechatronics*, vol. 25, no. 3, pp. 1193–1201, 2020.

[11] V. Guelpa, G. J. Laurent, P. Sandoz, J. G. Zea, and C. Clévy, "Subpixelic measurement of large 1d displacements: principle, processing algorithms, performances and software," *Sensors*, vol. 14, no. 3, pp. 5056–5073, 2014.

[12] L. Iafolla, L. Witthauer, A. Zam, G. Rauter, and P. C. Cattin, "Proof of principle of a novel angular sensor concept for tracking systems," *Sensors and Actuators A: Physical*, vol. 280, pp. 390–398, 2018.

[13] H. Yu, Q. Wan, Z. Mu, Y. Du, and L. Liang, "Novel nano-scale absolute linear displacement measurement based on grating projection imaging," *Measurement*, vol. 182, p. 109738, 2021.